Fluid Phase Equilibria 297 (2010) 90–97

Contents lists available at ScienceDirect

Fluid Phase Equilibria

journal homepage: www.elsevier.com/locate/fluid

Improvements of COSMO-SAC for vapor–liquid and liquid–liquid equilibrium predictions

Chieh-Ming Hsieh[a,b], Stanley I. Sandler[b], Shiang-Tai Lin[a,*]

[a] Department of Chemical Engineering, National Taiwan University, Taipei 10617, Taiwan
[b] Center for Molecular and Engineering Thermodynamics, Department of Chemical Engineering, University of Delaware, Newark 19716, DE, United States

ARTICLE INFO

Article history:
Received 1 May 2010
Received in revised form 17 June 2010
Accepted 19 June 2010
Available online 30 June 2010

Keywords:
COSMO-SAC
Vapor–liquid equilibria
Liquid–liquid equilibria
Prediction
Solvation

ABSTRACT

The COSMO-SAC model has been revised for a better description of the nonideality of liquid mixtures, and thus more accurate predictions of both vapor–liquid equilibrium (VLE) and liquid–liquid equilibrium (LLE). Two major modifications are introduced. First, the electrostatic interaction parameter is made temperature-dependent, which is important in LLE predictions for non-hydrogen-bonding systems. Second, the variation in the strength of hydrogen-bonding interactions involving different types of functional groups is treated using separate sigma-profiles. The overall RMS error in LLE predictions of 278 binary mixtures (4281 data points) from the new model is 0.1047, which is 30% lower than that from the original COSMO-SAC (0.1446), 10% lower from that of UNIFAC-LLE (0.1161), and comparable to that from the modified UNIFAC model (0.1048). The accuracy in VLE predictions is also improved. The average deviation in total pressure at a fixed liquid composition is 6.54% and the overall average deviation in vapor phase composition is 2.57% for 1338 binary mixtures, compared to 7.25% and 2.83% from the original model.

1. Introduction

The thermodynamic properties and phase behaviors of mixture fluids are very important in chemical and pharmaceutical industry [1–5], especially for the design and optimization of separation/purification processes. While it may be straightforward to acquire the needed data directly from experimental measurement, a reliable predictive model can significantly reduce the time, cost, and risk for problems involving extreme operation conditions and/or toxic chemicals.

Many predictive approaches have been developed over the past few decades, such as the group contribution methods (GCM) [6–15], quantitative structure property relationships (QSPR) [16–20], and artificial neural networks [21–23]. The success of these methods is often based on the number of experimental data used to evaluate the (tens or hundreds of) model parameters. Due to their simplicity and accuracy, GCMs, such as UNIFAC [2,24,25] and modified UNIFAC [26–28], have gained much popularity and been included in processes simulators [29]. However, the applicability of GCM can suffer from missing parameters for new, multifunctional chemicals [26].

In the past two decades, a new class of predictive methods has emerged that utilizes the results from modern computational chemistry. For example, the COSMO-based methods, such as the COSMO-RS [30–32], and its variations COSMO-SAC [33–35] and COSMO-RS(OI) [36], determine the liquid phase nonideality using the molecular interactions derived from first-principles solvation calculations [32,37]. This type of models does not contain any species-dependent parameters, and thus does not suffer from the problem of missing parameters. The COSMO-SAC model has been proven to provide acceptable predictions for the vapor pressures and normal boiling points of pure substances [34,38] and vapor–liquid equilibrium (VLE) of mixtures [33,35] (though not as good as GCMs with their hundreds of parameters). However, Hsieh and Lin [39] recently reported poor accuracy from COSMO-SAC for the description of liquid–liquid equilibrium (LLE).

In this work, we report a revision the COSMO-SAC model that improves the accuracy in predictions of both VLE and LLE. The weakness of the original COSMO-SAC model is analyzed using mixtures with and without hydrogen bonding. It is found that the use of a temperature-dependent electrostatic interaction parameter is critical to properly describe the LLE of non-hydrogen-bonding systems. For hydrogen-bonding mixtures we have found that it is important to account for the difference in the strength of hydrogen bond formed for specific donor–acceptor pairs. Here the species independent, universal parameters are determined using a small set of experimental LLE data, and it is found that the resulting model

* Corresponding author. Tel.: +886 2 3366 1369; fax: +886 2 2362 3040.
E-mail address: stlin@ntu.edu.tw (S.-T. Lin).

0378-3812/$ – see front matter © 2010 Elsevier B.V. All rights reserved.
doi:10.1016/j.fluid.2010.06.011

is more accurate than the original COSMO-SAC for both VLE and LLE predictions, and is comparable to the modified UNIFAC model in the prediction of LLE.

2. Theory

2.1. COSMO-SAC model

In the original COSMO-SAC model [10,35,40] the activity coefficient $\gamma_{i/S}$ of solute i in the solution S is determined from:

$$\ln \gamma_{i/S} = \frac{\Delta \underline{G}^{*res}_{i/S} - \Delta \underline{G}^{*res}_{i/i}}{RT} + \ln\ \gamma^{comb}_{i/S} \tag{1}$$

where $\Delta \underline{G}^{*res}$ is the restoring solvation free energy; the superscript *comb* denotes the combinatorial contribution, which is used to account for molecular size and shape differences between the species. In this work, the Staverman–Guggenheim combinatorial term is used.

$$\ln \gamma^{comb}_{i/S} = \ln \frac{\phi_i}{x_i} + \frac{z}{2} q_i\ \ln \frac{\theta_i}{\phi_i} + l_i - \frac{\phi_i}{x_i} \sum_j x_j l_j \tag{2}$$

with $\theta_i = (x_i q_i / (\sum_j x_j q_j))$, $\phi_i = (x_i r_i / (\sum_j x_j r_j))$, $l_i = (z/2)(r_i - q_i) - (r_i - l)$, where r_i and q_i are the normalized volume and surface area parameters for component i; x_i is the mole fraction of component i; z is the coordination number and is taken to be 10; the summation is over all the species in the mixture.

The restoring solvation free energy accounts for nonideality due to the difference in molecular interactions. In the COSMO-SAC model molecular interactions are calculated from the interaction between the surface screening charges when the molecules are in close contact. The screening charges can be obtained from first-principles solvation calculation of the molecule in a perfect conductor (infinite dielectric constant), a.k.a. the COSMO calculation [32]. In the COSMO calculation, the surface of a molecule is dissected to small segments and the screening charges are determined for each segment such that the net potential everywhere at the surface is zero (perfect screening). These charges are averaged to obtained the apparent screening charges to be used in the COSMO-SAC model:

$$\sigma_m = \frac{\sum_n \sigma^*_n \frac{r^2_n r^2_{\text{eff}}}{r^2_n + r^2_{\text{eff}}} \exp\left(-f_{decay} \frac{d^2_{mn}}{r^2_n + r^2_{\text{eff}}}\right)}{\sum_n \frac{r^2_n r^2_{\text{eff}}}{r^2_n + r^2_{\text{eff}}} \exp\left(-f_{decay} \frac{d^2_{mn}}{r^2_n + r^2_{\text{eff}}}\right)} \tag{3}$$

where σ and σ^* are charge density after and before charge averaging process; $\sigma_n = q_n/a_n$ is the charge density of segment (a_n is the surface area of the segment n); $r_n = \sqrt{a_n/\pi}$ is the radius of segment n; $r_{\text{eff}} = \sqrt{a_{\text{eff}}/\pi}$ is the radius of a standard surface segment; the empirical parameter f_{decay} has been set previously to 3.57 [41]; and d_{mn} is the distance between segments m and n.

The three-dimensional screening charge density distribution is quantified using a histogram known as σ-profile $p(\sigma)$, which is the probability of finding a surface segment with screening charge density σ. It is defined as

$$p_i(\sigma) = \frac{A_i(\sigma)}{A_i} \tag{4}$$

where $A_i(\sigma)$ is the surface area with a charge density of value σ, and A_i is the total surface area of species i. For a mixture, the σ-profile is determined from the area weighted average of contributions from all its components, i.e.

$$p_S(\sigma) = \frac{\sum_i x_i A_i p_i(\sigma)}{\sum_i x_i A_i} \tag{5}$$

In order to better describe hydrogen-bonding interactions Lin et al. [34] suggest separating the molecular surfaces into hydrogen-bonding ($A^{hb}_i(\sigma)$) and non-hydrogen-bonding ($A^{nhb}_i(\sigma)$) components, where $A^{hb}_i(\sigma)$ are the surfaces of oxygen, nitrogen, fluorine, and hydrogen atoms connected to a N, O, or F atom. Other surfaces are classified as $A^{nhb}_i(\sigma)$. The σ-profile then is

$$p_i(\sigma) = p^{nhb}_i(\sigma) + p^{hb}_i(\sigma) \tag{6}$$

with $p^{hb}_i(\sigma) = (A^{hb}_i(\sigma)/A_i) \times P^{HB}(\sigma)$ and $p^{nhb}_i(\sigma) = (A^{nhb}_i(\sigma)/A_i) + (A^{hb}_i(\sigma)/A_i) \times [1 - P^{HB}(\sigma)]$. $P^{HB}(\sigma)$ is a Gaussian-type function used to consider the probability of a *hb* segments in forming a hydrogen bond.

$$P^{HB}(\sigma) = 1 - \exp\left(\frac{\sigma^2}{2\sigma_0{}^2}\right) \tag{7}$$

where $\sigma_0 = 0.007$ e/Å^2 [33].

The activity coefficient (Γ) of segment m with a charge density of σ_m is determined from the σ-profile of the fluid:

$$\ln \Gamma^t_j(\sigma^t_m) = -\ln \left\{ \sum_s^{hb,\ nhb} \sum_{\sigma_n} p^s_j(\sigma^s_n) \Gamma^t_j(\sigma^s_n) \exp\left[\frac{-\Delta W(\sigma^t_m, \sigma^s_n)}{RT}\right] \right\} \tag{8}$$

where subscript j can either be the pure liquid (i) or a mixture (S); the superscript s and t can be either *hb* or *nhb*, representing the property for a hydrogen-bonding or non-hydrogen-bonding segment. The segment exchange energy is determined from the charge density of the interacting segments:

$$\Delta W(\sigma^t_m, \sigma^s_n) = c_{ES}(\sigma^t_m + \sigma^s_n)^2 - c_{hb}(\sigma^t_m, \sigma^s_n)(\sigma^t_m - \sigma^s_n)^2 \tag{9}$$

The c_{ES}, the electrostatic interaction parameter, is defined as

$$c_{ES} = f_{pol} \frac{0.3 a^{3/2}_{\text{eff}}}{2\varepsilon_0} \tag{10}$$

where $f_{pol} = 0.6916$ is the polarization factor [34] and ε_0 is the permittivity of vacuum. The hydrogen-bonding interaction parameter $c_{hb}(\sigma^t_m, \sigma^s_n)$ is given by

$$c_{hb}(\sigma^t_m, \sigma^s_n) = \begin{cases} c_{hb} & \text{if } s = t = hb \text{ and } \sigma^t_m \cdot \sigma^s_n < 0 \\ 0 & \text{otherwise} \end{cases} \tag{11}$$

The restoring free energy in Eq. (1) is obtained from:

$$\frac{\Delta \underline{G}^{*res}_{i/j}}{RT} = \frac{A_i}{a_{\text{eff}}} \sum_s^{nhb,\ hb} \sum_{\sigma_m} p^s_i(\sigma^s_m)\ \ln \Gamma^s_j(\sigma^s_m) \tag{12}$$

This version of COSMO-SAC was proposed by Wang et al. [33] and is referred to as original COSMO-SAC in this paper.

2.2. The revised COSMO-SAC model

Two modifications are introduced here to improve the performance of the model. First, the electrostatic interaction parameter c_{ES} is treated as a temperature-dependent parameter, i.e.,

$$c_{ES} = A_{ES} + \frac{B_{ES}}{T^2} \tag{13}$$

where A_{ES} and B_{ES} are universal constants whose values are listed in Table 1. Since A_{ES} and B_{ES} are positive numbers, c_{ES} decreases in value with increasing temperature and equals to the value used in original COSMO-SAC at $T = 273.14$ K. The replacement of Eq. (10) with Eq. (13) significantly improves the accuracy of liquid–liquid equilibrium (LLE) predictions for systems with no hydrogen-bonding interactions.

Table 1
Values of parameters in current COSMO-SAC model.

Universal parameters	
Parameter	Value
a_{eff} (Å^2)	7.25
f_{decay}	3.57
σ_0 (e/Å^2)	0.007
r (Å^3)	66.69
q (Å^2)	79.53
A_{ES} (kcal/mol)·(A^4/e^2)	6525.69
B_{ES} (kcal/mol)·(A^4/e^2)·K^2	1.4859×10^8
c_{OH-OH} (kcal/mol)·(A^4/e^2)	4013.78
c_{OT-OT} (kcal/mol)·(A^4/e^2)	932.31
c_{OH-OT} (kcal/mol)·(A^4/e^2)	3016.43

Atomic radii	
Atom type	Radius (Å)
H	1.30
C	2.00
N	1.83
O	1.72
F	1.72
Cl	2.05
Br	2.16
I	2.32
S	2.16
P	2.12

The second modification is introduced for systems containing hydrogen-bonding interactions. It has been experimentally discovered that the strength of a hydrogen bond varies with the substances that form it [42]. The original COSMO-SAC model, using only one $p^{hb}(\sigma)$, can not differentiate properly in the hydrogen-bonding energy, for example, between O. . .H and N. . .H. In this work, we propose to differentiate the surfaces on hydroxyl groups ($A_i^{OH}(\sigma)$, e.g., OH in water and alcohol) from other hydrogen-bonding surfaces ($A_i^{OT}(\sigma)$, e.g. O in ketones, NO_2 in nitro-compounds, and NH_2 in amines.). Therefore, we use for $p^{hb}(\sigma)$ in Eq. (6):

$$p_i^{hb}(\sigma) = p_i^{OH}(\sigma) + p_i^{OT}(\sigma) \tag{14}$$

with $p_i^{OH}(\sigma) = (A_i^{OH}(\sigma)/A_i) \times P^{HB}(\sigma)$ and $p_i^{nhb}(\sigma) = (A_i^{OT}(\sigma)/A_i) \times P^{HB}(\sigma)$. The σ-profiles of four selected compounds are illustrated in Fig. 1. As a result, it is necessary to define the interactions between surfaces *OH–OH*, *OT–OT*, and *OH–OT* in Eq. (9), i.e.,

$$c_{hb}(\sigma_m^t, \sigma_n^s) = \begin{cases} c_{OH-OH} & \text{if } s = t = OH \text{ and } \sigma_m^t \cdot \sigma_n^s < 0 \\ c_{OT-OT} & \text{if } s = t = OT \text{ and } \sigma_m^t \cdot \sigma_n^s < 0 \\ c_{OH-OT} & \text{if } s = OH,\ t = OT, \text{ and } \sigma_m^t \cdot \sigma_n^s < 0 \\ 0 & \text{otherwise} \end{cases} \tag{15}$$

The values of these three parameters were obtained from regression to experimental data, and their values are given in Table 1. A careful examination has been conducted and we conclude that differentiation of the hydrogen-bonding surface to more than the two types considered has only marginal effect in the accuracy of the model. (A brief summary of the analysis is provided in Supplementary Materials.) We also found that making c_{hb} temperature dependent did not improve the accuracy of the method.

3. Computational details

The procedure to calculate the activity coefficient from COSMO-SAC is as follows. The first step is to generate the *cosmo* files from DFT/COSMO calculation [32]. The detailed setting of DFT/COSMO calculation can be found elsewhere [35]. This is the most time-consuming step, but needs to be done only once for each compound,

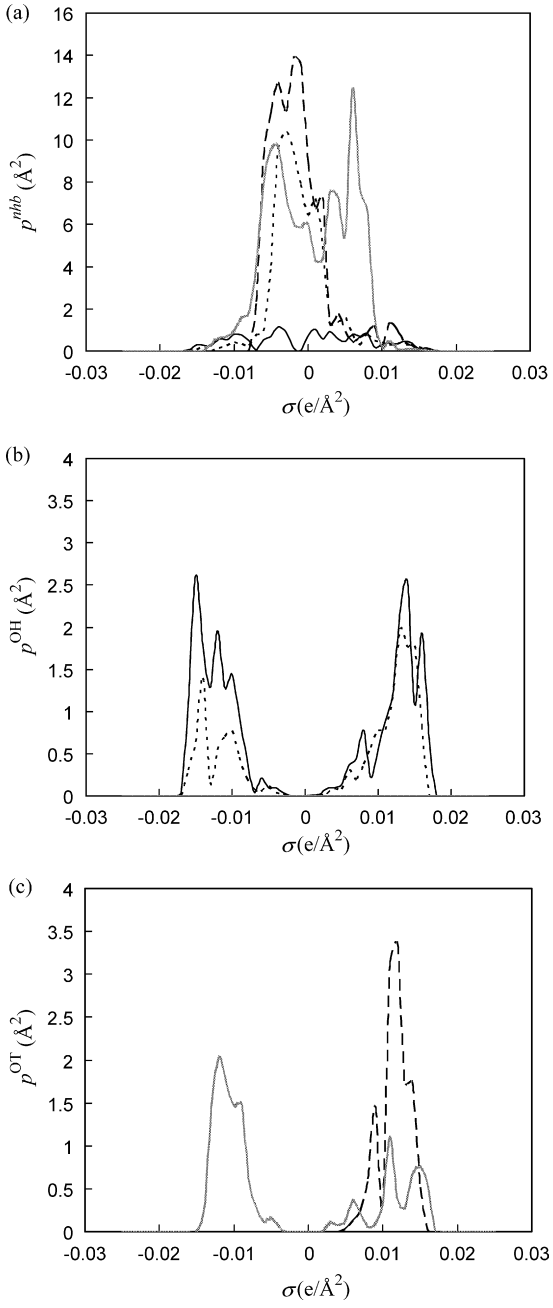

Fig. 1. The σ-profiles (multiplied by the surface area, A_i) for the (a) non-hydrogen-bonding component, (b) OH component, and (c) OT component of four selected compounds; ethanol (dotted lines), 2-butanone (dashed lines), water (solid line), and aniline (gray line). The summation of OH and OT σ-profiles is the hydrogen-bonding σ-profiles in the original COSMO-SAC [33].

and then stored in a database for all further use. A good example is the VT-database [43,44] from Liu's group at Virginia Tech that contains the *cosmo* files for over 1400 compounds and is freely available on the Internet. We have used the VT-database in this work. (Note that the VT-database was established using the quantum mechanical program, DMol^3 in Materials Studio [45]. Different QM packages may provide different *cosmo* files and a re-optimization of the parameters listed in Table 1 may be necessary [46,47].) For each component the screening charges in the *cosmo* files are averaged [Eq. (3)] and the σ-profile is created according to Eqs. (4), (6), or (14). The σ-profile of the mixture is then computed using Eq. (5). The segment activity coefficients for each pure liquid and mixture are calculated from Eq. (8). The restoring free energy can then be

Table 2
Comparison of RMS error of liquid–liquid equilibrium prediction from different predictive methods.

	N_{sys} (exp)	Revised COSMO-SAC		Original COSMO-SAC [33]		Modified UNIFAC [26]		UNIFAC-LLE [51]	
		N_{sys}	RMS	N_{sys}	RMS	N_{sys}	RMS	N_{sys}	RMS
Type I	71	55	0.1094	55	0.1464	55	0.1514	49	0.1952
Type II	85	79	0.0813	81	0.0891	74	0.0630	60	0.0459
Type III	122	109	0.1193	90	0.1936	96	0.1103	91	0.1198
Overall	278	243	0.1047	226	0.1446	225	0.1048	200	0.1161

obtained from Eq. (12) and the activity coefficients of each of the component in the mixture from Eq. (1).

4. Parameter optimization

There are a total of 10 parameters in the revised COSMO-SAC model, in addition to the atomic radii. Among them, 8 global parameters are used in the restoring free energy calculations (surface area of a standard segment a_{eff}, f_{decay}, and 6 parameters for the electrostatic and hydrogen-bonding interactions), and 2 (r and q) are used in the Staverman–Guggenheim combinatorial term. All the parameters are taken from original COSMO-SAC model [33], except for the 5 newly introduced parameters (A_{ES}, B_{ES}, c_{OH-OH}, c_{OH-OT}, and c_{OT-OT}), whose values were obtained from optimization using only experimental liquid–liquid equilibrium (LLE) data and the following objective function:

$$obj = \left[\frac{1}{M} \sum_{j=1}^{M} (x_j^{\text{calc}} - x_j^{\text{expt}})^2 \right]^{1/2} \tag{16}$$

where M is number of LLE data points; the superscripts calc and expt indicated the calculated results and the experimental data, respectively. All the experimental LLE data were retrieved from DECHEMA database.

The parameter optimization of these five parameters was performed as follows. First, A_{ES} and B_{ES} were optimized from 18 LLE systems in which there were no hydrogen-bonding (hb) interactions. Once the optimal values were found, they were fixed. Second, c_{OH-OH} and c_{OH-OT} were optimized using data for 39 LLE systems. Finally, c_{OT-OT} was optimized using data for an additional 17 LLE systems. The LLE systems used in optimization are summarized in Supplementary Materials and the values of the parameters are listed in Table 1. The values of hb interaction parameters shown in Table 1 are very different, an indication that the different types of hb interactions can be very different.

5. Results and discussions

The revised model is validated using both LLE (278 binary mixtures with temperatures ranging from 243.15 K to 483.45 K) and VLE (1338 binary mixtures with temperature ranging from 207.92 K to 553.15 and pressure from 0.112 kPa to 6.87 MPa) data. All the data are taken from the DECHEMA Chemistry Data Series [48,49]. To facilitate the analysis, the mixtures were categorized into three types [39,50]. Type I are the systems that do not have any hydrogen-bonding (hb) interactions, such as nitromethane + benzene and acetone + hexane. The type II systems include a compound that has an hb self-association, for example, water + hexane and ethylamine + benzene. In type III systems, both self- and cross-hb associations occur as in the water + acetone and nitromethane + ethylamine systems.

5.1. Liquid–liquid equilibria

Table 2 summarizes RMS errors in LLE predictions from 4 liquid models. The revised COSMO-SAC model is the most accurate, with the lowest RMS error of 0.1047, which is 28% less than that from original COSMO-SAC (0.1446) and similar to that from the modified UNIFAC [26] (0.1048) and UNIFAC-LLE [51] (0.1161) models. Furthermore, the revised COSMO-SAC model is most successful in terms predicting the presence of a miscibility gap in that 243 out of the 278 systems are predicted to exhibit LLE, where as only 226 from the original COSMO-SAC, 225 from modified UNIFAC and only 200 from UNIFAC-LLE. Note that here a system is a set of LLE data for a specific binary mixture. The reason for a model failing to predict the presence of a miscible gap may be (1) the mixture is

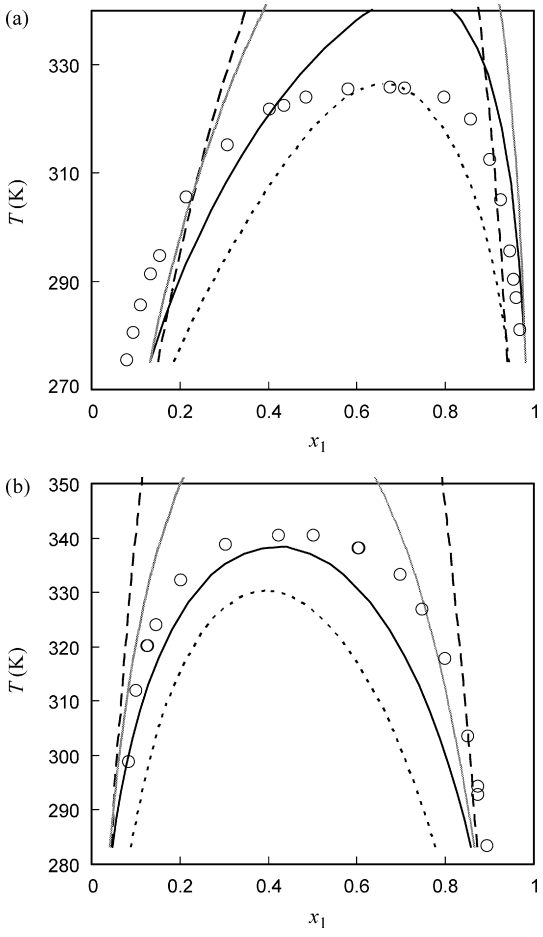

Fig. 2. Comparison of the liquid–liquid equilibrium predictions with experiment data for systems with no hydrogen-bonding interactions (type I systems) (a) (1) nitroethane + (2) n-decane and (b) (1) furfural + (2) methylcyclopentane. The open circles are the experimental data taken from Sørensen and Arlt [49]. The solid lines, gray lines, dotted lines, and dashed lines are the predictions from revised COSMO-SAC, original COSMO-SAC [33], modified UNIFAC [26], and UNIFAC-LLE [51] models, respectively.

predicted to be completely miscible, (2) the temperature is above the predicted upper critical solution temperature of the model, or (3) simply missing of necessary parameters as is the case for the modified UNIFAC and UNIFAC-LLE models.

The revised COSMO-SAC model provides the lowest RMS error for type I systems, a 25% decrease from original COSMO-SAC. Since there are no *hb* interactions in type I systems, the improvement seen here is a result of the use of a temperature-dependent electrostatic interaction [i.e., Eq. (13) vs. Eq. (10)]. As illustrated in Fig. 2, the temperature dependence of miscible gap of these two systems is well described by modified COSMO-SAC. UNIFAC-LLE is the least accurate model for type I systems. The possible reason is that its binary interaction parameters were optimized using mostly LLE data around ambient temperature. Gupte and Danner [52] have systematically evaluated the accuracy of UNIFAC-LLE in LLE predictions of binary and ternary mixtures and suggested to use it only within a small temperature range from 10 to 40 °C.

The RMS errors from all approaches are relatively smaller for type II systems. The *hb* compounds and *nhb* compounds are very dissimilar, and therefore most models can easily describe the existence of LLE. Note that about one-third of systems classified in type II are water + hydrocarbons (including chloro-hydrocarbons). All 4 methods describe such systems well. The UNIFAC-LLE is the most accurate model, but it can be used for predictions for the fewest systems because of missing parameters. Due to the use of temperature-dependent electrostatic interaction, the revised COSMO-SAC model results a better description of the temperature dependence of the miscible gap for type II systems (as illustrated in Fig. 3).

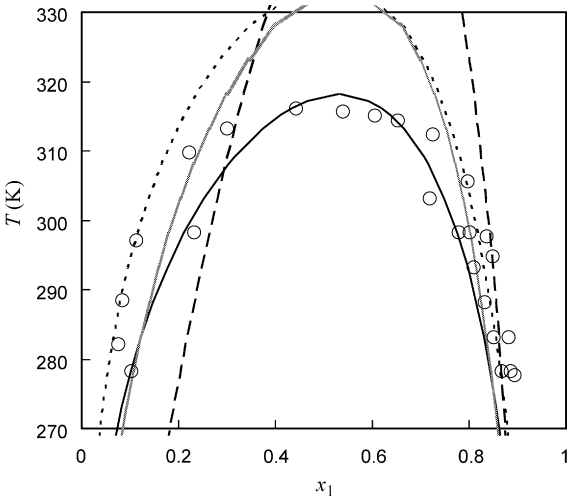

Fig. 3. Comparison of the liquid–liquid equilibrium predictions with experiment data for the system (1) methanol + (2) n-hexane (type II system). The legends are the same as in Fig. 2 and the experimental data are taken from Sørensen and Arlt [49].

The prediction of LLE in type III systems is most challenging because it requires an accurate description of the subtle differ-

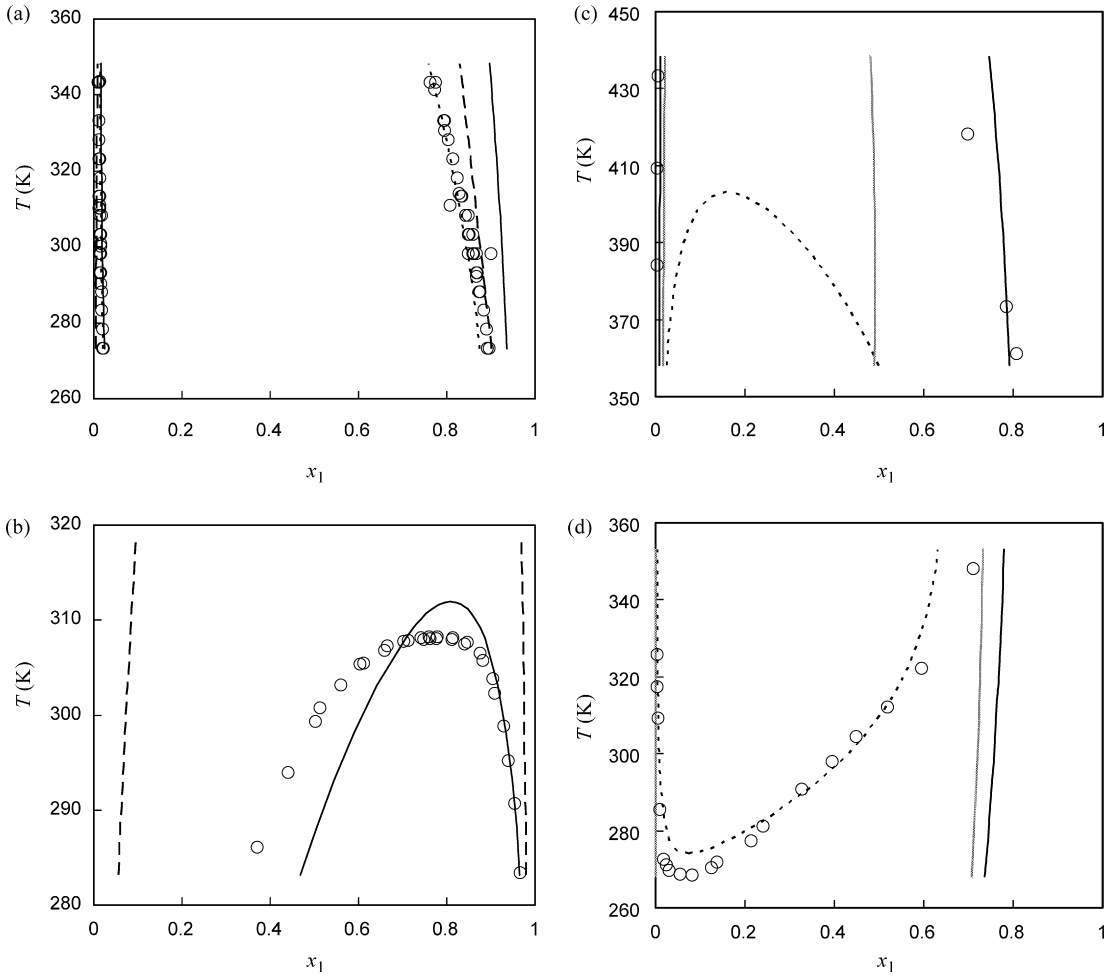

Fig. 4. Comparison of the liquid–liquid equilibrium predictions with experiment data for systems having self- and cross-hydrogen-bonding interactions (type III systems) (a) (1) ethyl acetate + (2) water, (b) (1) nitromethane + (2) n-octanoic acid, (c) (1) p-chloroaniline + (2) water, and (d) (1) di-n-proplyamine + (2) water. The legends are the same as in Fig. 2 and the experimental data are taken from Sørensen and Arlt [49].

Table 3
Comparison of overall deviation of binary VLE.

	N_{sys}[a]	Revised COSMO-SAC		Original COSMO-SAC [33]		N_{sys}[b]	Modified UNIFAC [26]	
		AARD-P (%)	AAD-y_1 (%)	AARD-P (%)	AAD-y_1 (%)		AARD-P (%)	AAD-y_1 (%)
Type I	638	4.31	1.66	4.43	1.71	554	1.86	0.92
Type II	309	8.34	3.03	9.67	3.25	305	2.74	1.56
Type III	391	8.73	3.68	9.94	4.33	383	4.79	2.40
Overall	1338	6.54	2.57	7.25	2.83	1242	2.98	1.53

[a] The number of VLE systems considered and described by original and revised COSMO-SAC model in this study.
[b] The number of these VLE systems that can be described by modified UNIFAC.

ences in the *hb* interactions among all the species pairs. As shown in Table 2, when compared with original COSMO-SAC, the RMS error from revised COSMO-SAC is reduced by 38% and the number of systems that are successfully described miscible gaps increases from 90 to 109. Fig. 4a and b are examples in which the revised COSMO-SAC model predicts the existence of LLE but the original COSMO-SAC model does not. In addition, the performance of the revised model for systems containing amines is slightly improved, as shown in Fig. 4c and d. Therefore, we conclude that the distinction of *hb* interactions [Eq. (15)] is very effective for type III systems. The modified UNIFAC model gives the lowest RMS error and sometimes results in better prediction of the temperature dependence of miscible gap (as shown in Fig. 4a and d). However, this model and UNIFAC-LLE is limited in its applicability by the availability of binary interaction parameters and the appropriate group definitions. For example, the modified UNIFAC model cannot describe the system in Fig. 4b because the necessary parameters for nitro and carboxylic groups are unavailable. The situation is similar in Fig. 4c for UNIFAC-LLE, where the parameters of amino groups are not available. Both the COSMO-SAC models do not suffer from that problem.

It is useful to point out some limitations of the revised COSMO-SAC model in LLE predictions. The first and most important is that it cannot correctly describe lower critical solution temperature (LCST). Fig. 4d illustrates the presence LCST in the mixture of di-n-propylamine and water. The modified UNIFAC can successfully predict the LCST. While the revised COSMO-SAC predicts the closing of miscible gap with decreasing temperature, its LCST is much too low. Secondly, the COSMO-SAC may fail to describe a system containing flexible molecules without a more careful treatment. Good examples are systems containing glycerol. Only 1 out of 9 systems containing glycerol was successfully predicted to show LLE (see Supplementary Materials). While conformation is quite important [3,53,54], we consider it as a different issue and is beyond the scope of the present study.

5.2. Vapor–liquid equilibria

While the 5 new parameters introduced in this work are obtained from fitting to LLE data, it is interesting to show that the accuracy of the revised COSMO-SAC model for VLE is also improved. The accuracy is evaluated using the average absolute relative deviation in pressure (AARD-P):

$$\text{AARD-}P\,(\%) = \frac{1}{M}\sum_{i=1}^{M}\frac{\left|P_i^{\text{calc}} - P_i^{\text{expt}}\right|}{P_i^{\text{expt}}} \times 100 \tag{17}$$

and average absolute deviation in vapor phase composition (AAD-y_1):

$$\text{AAD-}y_1\,(\%) = \frac{1}{M}\sum_{i=1}^{M}\left|y_{1,i}^{\text{calc}} - y_{1,i}^{\text{expt}}\right| \times 100 \tag{18}$$

where M is the number of data points within a binary mixture; superscript calc and expt are the predictions and experimental data, respectively. As shown in Table 3, the overall AARD-P and AAD-y_1 from the revised COSMO-SAC model are 6.54% and 2.83%, respectively. Both of these errors are reduced by almost 10% compared to those from the original model. The predicted results from revised COSMO-SAC are better than those from original COSMO-SAC for type I and II systems; and their accuracies are similar for type III systems. For some type I systems (no *hb* interactions), the improvement is very significant. As a reference, the predictions from the modified UNIFAC model [26] are also listed in Table 3. The modified UNIFAC model is the most accurate method, with the overall AARD-P and AAD-y_1 being 2.93% and 1.53%, respectively. (Note that fewer systems are considered with modified UNIFAC because of missing

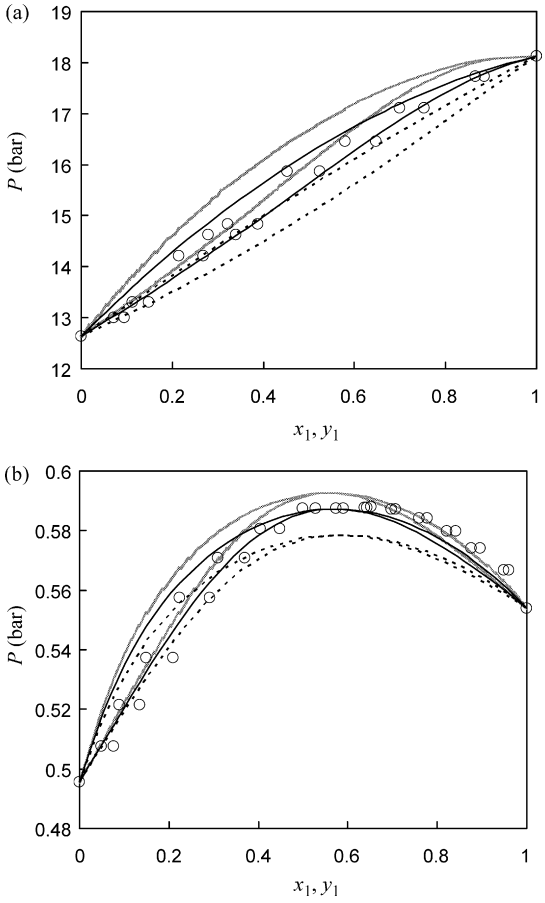

Fig. 5. Comparison of the vapor–liquid equilibrium predictions with experiment data for systems with no hydrogen-bonding interactions (type I systems) (a) (1) benzene + (2) n-heptane at 488.15 K and (b) (1) ethyl acetate + (2) acetonitrile at 333.15 K. The open circles are experimental data taken from Gmehling et al. [48]. The solid lines, gray lines, and dotted lines are predicted results from revised COSMO-SAC, original COSMO-SAC [33], and modified UNIFAC [26], respectively.

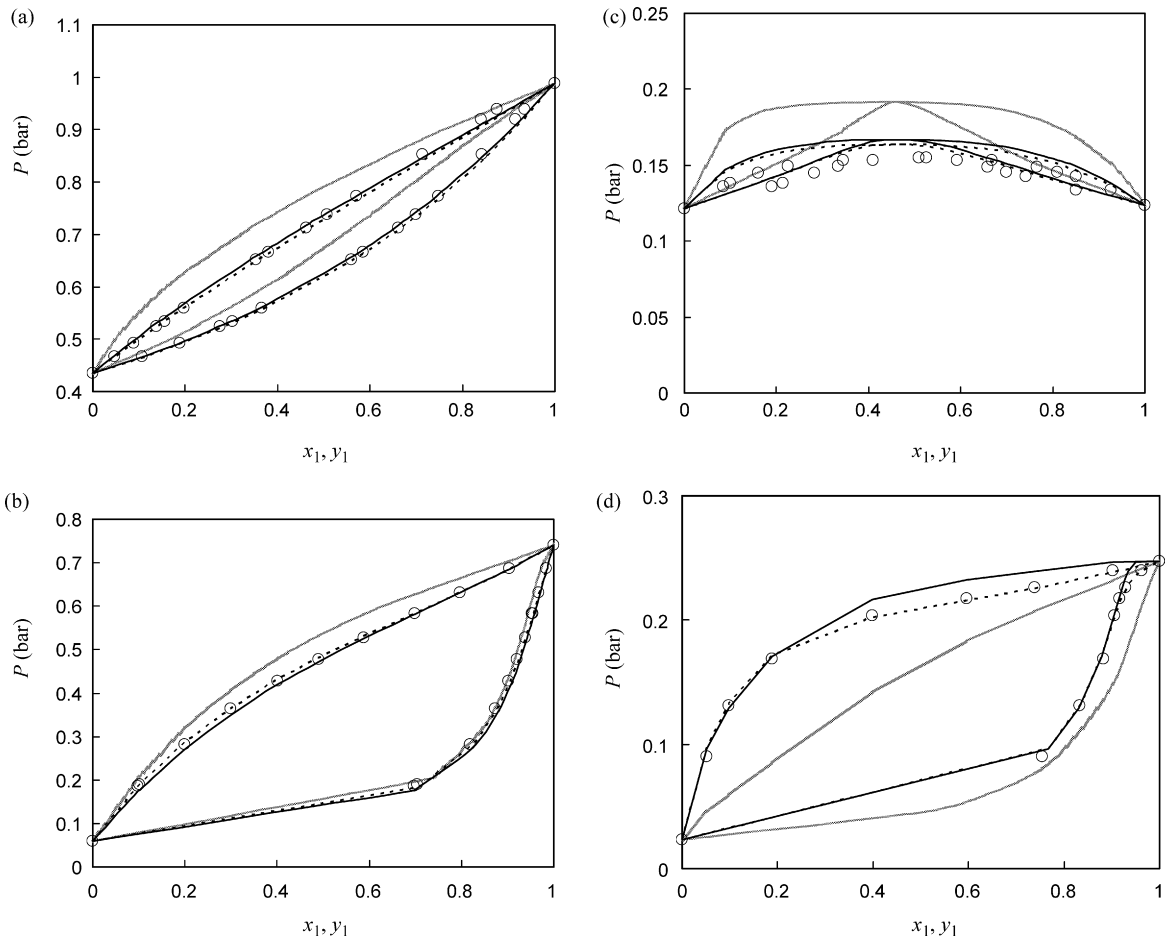

Fig. 6. Comparison of the vapor–liquid equilibrium predictions with experiment data for hydrogen-bonding systems (a) (1) di-ethylamine + (2) benzene at 328.15 K (type II systems), (b) (1) toluene + (2) aniline at 373.17 K (type II systems), (c) (1) n-butylamine + (2) acetonitrile at 298.15 K (type III systems), and (d) (1) acetone + (2) water at 293.15 K (type III systems). The legends are the same as in Fig. 5 and the experimental data are taken from Gmehling et al. [48].

functional group parameters [26] for some species.) Fig. 5 shows the VLE of one system at high temperature (488.15 K) and one system at a lower temperature (333.15 K). In both cases, the revised model is clearly more accurate than the original model. This again supports the use of temperature-dependent electrostatic interactions [Eq. (13)]. For systems having *hb* interactions, i.e. types II and III systems, significant improvement is also found as illustrated in Fig. 6, especially for systems containing amino group (–NH_2 or –NH) (Fig. 6a–c). The improved accuracy in VLE predictions of the revised COSMO-SAC model is due to the two modifications made in this work.

6. Conclusion

Two modifications have been introduced into the COSMO-SAC model to improve its accuracy in both liquid–liquid equilibrium (LLE) and vapor–liquid equilibrium (VLE) predictions. Making the electrostatic interaction parameter temperature-dependent is found to be very effective in improving LLE predictions for non-hydrogen-bonding systems. In addition, the variation of hydrogen-bonding strength for different donor–acceptor pairs is taken into account. This is realized by the separation of the hydrogen-bonding surfaces, and hence the σ-profile, in to those involving OH groups and separately from all others. The 5 parameters [two electrostatic interaction parameters (A_{ES} and B_{ES}) and three hydrogen-bonding interaction parameters (c_{OH-OH}, c_{OH-OT}, and c_{OT-OT})] introduced as a result of these modifications are determined by regression using a small set of LLE data. The revised model is much more accurate than the original one for the description LLE, and its accuracy is comparable to that from the modified UNIFAC. More importantly, the performance of the revised model for VLE is also improved. Therefore, the revised model is a more accurate method for both VLE and LLE predictions when no experimental data are available.

Acknowledgement

The authors would like to thank the financial support from NSC 98-2221-E-002-087-MY3 and NSC 97-2917-I-002-118 by the National Science Council of Taiwan and computation resources from the National Center for High-Performance Computing of Taiwan.

Appendix A. Supplementary data

Supplementary data associated with this article can be found, in the online version, at doi:10.1016/j.fluid.2010.06.011.

References

[1] S.J. Wang, C.C. Yu, H.P. Huang, Comput. Chem. Eng. 34 (2010) 361–373.
[2] A. Fredenslund, J. Gmehling, M.L. Michelsen, P. Rasmussen, J.M. Prausnitz, Ind. Eng. Chem. Process Des. Dev. 16 (1977) 450–462.
[3] T. Banerjee, R.K. Sahoo, S.S. Rath, R. Kumar, A. Khanna, Ind. Eng. Chem. Res. 46 (2007) 1292–1304.
[4] S.I. Sandler, Chemical and Engineering Thermodynamics, 3rd ed., John Weily & Sons, New York, 1999.

[5] J.M. Prausnitz, R.N. Lichtenthaler, E.G. de Azevedo, Molecular Thermodynamics of Fluid-Phase Equilibria, 3rd ed., Pearson Education Taiwan Ltd, Taipei, 2004.
[6] B.E. Poling, J.M. Prausnitz, J.P. O'Connell, The Properties of Gases and Liquids, 5th ed., McGraw-Hill, New York, 2001.
[7] A. Diedrichs, J. Rarey, J. Gmehling, Fluid Phase Equilib. 248 (2006) 56–69.
[8] S.T. Lin, S.I. Sandler, Chem. Eng. Sci. 57 (2002) 2727–2733.
[9] S.T. Lin, S.I. Sandler, J. Phys. Chem. A 104 (2000) 7099–7105.
[10] S.T. Lin, S.I. Sandler, Ind. Eng. Chem. Res. 38 (1999) 4081–4091.
[11] S.J. Zhang, T. Hiaki, M. Hongo, K. Kojima, Fluid Phase Equilib. 144 (1998) 97–112.
[12] T. Holderbaum, J. Gmehling, Fluid Phase Equilib. 70 (1991) 251–265.
[13] J. Marrero, R. Gani, Fluid Phase Equilib. 183 (2001) 183–208.
[14] L. Constantinou, R. Gani, J.P. Oconnell, Fluid Phase Equilib. 103 (1995) 11–22.
[15] L. Constantinou, R. Gani, AIChE J. 40 (1994) 1697–1710.
[16] F.A.D. Ribeiro, M.M.C. Ferreira, Theochem. J. Mol. Struct. 663 (2003) 109–126.
[17] S.S. Godavarthy, R.L. Robinson, K.A.M. Gasem, Fluid Phase Equilib. 246 (2006) 39–51.
[18] A.R. Katritzky, S.H. Slavov, D.A. Dobchev, M. Karelson, Comput. Chem. Eng. 31 (2007) 1123–1130.
[19] D. Ravindranath, B.J. Neely, R.L. Robinson, K.A.M. Gasem, Fluid Phase Equilib. 257 (2007) 53–62.
[20] D. Sola, A. Ferri, M. Banchero, L. Manna, S. Sicardi, Fluid Phase Equilib. 263 (2008) 33–42.
[21] C.I. Anghel, M.V. Cristea, Rev. Chim. 61 (2010) 87–93.
[22] R. Sharma, D. Singhal, R. Ghosh, A. Dwivedi, Comput. Chem. Eng. 23 (1999) 385–390.
[23] E. Alvarez, C. Riverol, J.M. Correa, J.M. Navaza, Ind. Eng. Chem. Res. 38 (1999) 1706–1711.
[24] H.K. Hansen, P. Rasmussen, A. Fredenslund, M. Schiller, J. Gmehling, Ind. Eng. Chem. Res. 30 (1991) 2352–2355.
[25] S. Skjoldjorgensen, B. Kolbe, J. Gmehling, P. Rasmussen, Ind. Eng. Chem. Process Des. Dev. 18 (1979) 714–722.
[26] J. Gmehling, J. Lohmann, A. Jakob, J.D. Li, R. Joh, Ind. Eng. Chem. Res. 37 (1998) 4876–4882.
[27] J. Gmehling, J.D. Li, M. Schiller, Ind. Eng. Chem. Res. 32 (1993) 178–193.
[28] U. Weidlich, J. Gmehling, Ind. Eng. Chem. Res. 26 (1987) 1372–1381.
[29] Aspen Plus Unit Operation Models, Aspen Technology Inc, Burlington, MA, 2007.
[30] A. Klamt, V. Jonas, T. Burger, J.C.W. Lohrenz, J. Phys. Chem. A 102 (1998) 5074–5085.
[31] A. Klamt, J. Phys. Chem. 99 (1995) 2224–2235.
[32] A. Klamt, G. Schuurmann, J. Chem. Soc. Perkin Trans. 2 (1993) 799–805.
[33] S. Wang, S.I. Sandler, C.C. Chen, Ind. Eng. Chem. Res. 46 (2007) 7275–7288.
[34] S.T. Lin, J. Chang, S. Wang, W.A. Goddard, S.I. Sandler, J. Phys. Chem. A 108 (2004) 7429–7439.
[35] S.T. Lin, S.I. Sandler, Ind. Eng. Chem. Res. 41 (2002) 899–913.
[36] H. Grensemann, J. Gmehling, Ind. Eng. Chem. Res. 44 (2005) 1610–1624.
[37] S.T. Lin, C.M. Hsieh, J. Chem. Phys. 125 (2006).
[38] S. Wang, S.T. Lin, J. Chang, W.A. Goddard, S.I. Sandler, Ind. Eng. Chem. Res. 45 (2006) 5426–5434.
[39] C.M. Hsieh, S.T. Lin, Chem. Eng. Sci. 65 (2010) 1955–1963.
[40] S.T. Lin, S.I. Sandler, AIChE J. 45 (1999) 2606–2618.
[41] S.T. Lin, S.I. Sandler, Ind. Eng. Chem. Res. 43 (2004) 1322–11322.
[42] G.C. Pimentel, A.L. McClellan, The Hydrogen Bond, W. H. Freeman and Company, New York, 1960.
[43] E. Mullins, R. Oldland, Y.A. Liu, S. Wang, S.I. Sandler, C.C. Chen, M. Zwolak, K.C. Seavey, Ind. Eng. Chem. Res. 45 (2006) 4389–4415.
[44] E. Mullins, Y.A. Liu, A. Ghaderi, S.D. Fast, Ind. Eng. Chem. Res. 47 (2008) 1707–1725.
[45] DMol^3, Materials Studio, Accelrys Software Inc., San Diego, CA, 2005.
[46] T.C. Mu, J. Rarey, J. Gmehling, AIChE J. 53 (2007) 3231–3240.
[47] T.C. Mu, J. Rarey, J. Gmehling, Ind. Eng. Chem. Res. 46 (2007) 6612–6629.
[48] J. Gmehling, U. Onken, W. Arlt, Vapor–liquid Equilibrium Data Collection, Dechema, Frankfurt, 1977.
[49] J.M. Sørensen, W. Arlt, Liquid-Liquid Equilibrium Data Collection, Dechema, Frankfurt, 1979.
[50] G.N. Escobedo-Alvarado, S.I. Sandler, AIChE J. 44 (1998) 1178–1187.
[51] T. Magnussen, P. Rasmussen, A. Fredenslund, Ind. Eng. Chem. Process Des. Dev. 20 (1981) 331–339.
[52] P.A. Gupte, R.P. Danner, Ind. Eng. Chem. Res. 26 (1987) 2036–2042.
[53] S. Wang, J.M. Stubbs, J.I. Siepmann, S.I. Sandler, J. Phys. Chem. A 109 (2005) 11285–11294.
[54] A. Klamt, COSMO-RS from Quantum Chemistry to Fluid Phase Thermodynamics and Drug Design, Elsevier, Amsterdam, 2005.